Integration of Global Positioning System and Scanning Water Vapor Radiometers for Precipitable Water Vapor and Cloud Liquid Path Estimates

V. Mattioli and P. Basili
Department of Electronic and Information Engineering
University of Perugia
Perugia, Italy

E. R. Westwater
Cooperative Institute for Research in Environmental Sciences
University of Colorado
National Oceanic and Atmospheric Administration
Environmental Technology Laboratory
Boulder, Colorado

Introduction

In recent years the Global Positioning System (GPS) has proved to be a reliable instrument for measuring precipitable water vapor (PWV) (Bevis et al. 1992), offering an independent source of information on water vapor when compared with microwave radiometers (MWRs), and/or radiosonde observations (RAOBs) (Rocken et al. 1995, Basili et al. 2001). In our work we compared PWV from MWRs, GPS, and RAOBs examining in detail several assumptions in water vapor estimation. The objective was to combine GPS with MWR observations to get retrievals of cloud liquid path (CLP) that may be improvements over those obtained with MWR alone. We evaluated this method from data collected during the Cloudiness Inter-Comparison (CIC) Experiment intensive operational period (IOP) that was conducted at the Atmospheric Radiation Measurement (ARM) Program's Southern Great Plains site (SGP) in North-Central Oklahoma. The SGP is a field measurement site consisting of a variety of in situ and remote-sensing instruments and is a powerful source for testing and analyzing concurrent data from different instruments. The instruments we considered in our work were three dual-channel scanning MWRs operated by ARM, the SuomiNet Ground-Based GPS operated by the National Oceanic and Atmospheric Administration/Forecast Systems Laboratory (NOAA/FSL) at the same site, and RAOBs, with the Vaisala RS90 humidity sensor, launched four times a day. Soundings from all of these sources were compared during the CIC-IOP. Clear and cloudy conditions were identified by use of ARM operational cloud-boundary products derived from lidar and cloud radar. Combined GPS and MWR measurements were considered for the retrieval of PWV and CLP for both clear and cloudy datasets. Good general agreement in the PWV measurement was found between the three different kinds of instruments, with root mean square (rms) differences of 1 to 2 mm. We focused our analysis on cloudy conditions to investigate a possible dependence of the PWV differences on meteorological conditions as well as on water vapor amount itself. This comparison offered the opportunity of testing the reliability of these instruments in the presence of clouds.

PWV and CLP Retrieval

During the CIC IOP, in March and April 2003, two MWRs supplemented for the operational SGP central facility MWR. The three MWRs were dual-channel water vapor radiometers operating with sampling time of one minute at 23.8 and 31.4 GHz. The half power beamwidth of the two channels is 5.9 and 4.5 degrees, respectively. The operational SGP C1 scans at five angles (19.35, 23.4, 30.15, 41.85, and 90.0 degrees) in east-west direction, and the two additional E14 and S01 scanned correspondingly in the same vertical plane and in the orthogonal plane (north-south) as that of operational unit.

A GPS permanent station, belonging to the Suominet network and managed by the University Corporation for Atmospheric Research (UCAR) and the NOAA/FSL, is operating with co-located surface meteorological sensors at SGP site. The system currently provides PWV estimates every 30 minutes with less than 25 minute latency.

PWV and CLP from MWR

It is well known (Westwater 1993) that it is possible to retrieve water vapor and liquid water considering brightness temperatures T_Bs measured by a ground-based MWR at 23.8 GHz and at 31.4 GHz. The first frequency is sensitive to the water vapor because of its nearness to the 22.235 GHz H_2O absorption line, and the other, in a clear-air window, is more responsive to the liquid water. Sky equivalent T_Bs provided by the radiometer are given in Eq. 1 (Liljegren 2000):

$$T_B = T_{ref} + \frac{f_w T_{nd}}{(V_{ref+nd} - V_{ref})}(V_{sky} - V_{ref}) \quad (1)$$

where T_{ref} is the reference target absolute temperature, f_w is the polycarbonate foam window loss factor, T_{nd} the noise diode injection temperature; V_{sky} and V_{ref} are the output signal when the radiometer is looking at the sky and at the reference target respectively and V_{ref+nd} the signal when the radiometer is looking at the reference target and the signal from the noise diode is injected.

The T_B observed at zenith, at frequency f, is defined by Eq. 2 (Westwater 1993), assuming non-scattering atmosphere in local thermodynamic equilibrium, so that each air volume at point z can be characterized by a temperature T(z):

$$T_B(f) = T_C\ e^{-\tau_f(0,\infty)} + \int_0^\infty T(z)\,\alpha(f,z) e^{-\tau_f(0,z)} dz \quad (2)$$

where T_C is the cosmic background, $\alpha(f,z)$ is the atmospheric absorption coefficient, $\tau_f(0,\infty)$ is the atmospheric opacity and $\tau_f(0,z)$ the optical depth. To retrieve water vapor and liquid water T_Bs are usually converted into the atmospheric opacities τ_f, by means of the mean radiating temperature $T_{mr}(f)$ (Westwater 1993), as in Eq. 3:

$$\tau_f = \ln\left(\frac{T_{mr}(f) - T_C}{T_{mr}(f) - T_B(f)}\right) \quad (3)$$

PWV and CLP are then estimated as shown in Eqs. 4 and 5:

$$PWV = a_0 + a_1\tau_{23} + a_2\tau_{31} \quad (4)$$

$$CLP = b_0 + b_1\tau_{23} + b_2\tau_{31} \quad (5)$$

Retrieval coefficients a_i and b_i were estimated by linear regression for each month on the basis of 10 years of RAOB data launched at the SGP.

In our work we evaluated two calibrations for the MWRs, the ARM automatic self-calibration (Liljegren 2000) and the Environmental Technology Laboratory (ETL) tipping calibration method (Han and Westwater 2000). Both algorithms involve tip curves, that are measurements of opacity at different elevation angles as a function of air mass, defined as the ratio of the opacity at a direction θ, and the opacity at zenith. ARM MWRs elevation angles are close to air mass 3, 2.5, 2, 1.5, and 1.

The ETL method is based on instantaneous tip curves, deriving for each tip the gain correction $f_w T_{nd}$ in Eq. (1), measurements at angles on both sides of zenith used to assure horizontal homogeneity under the assumption of stratified atmosphere.

In contrast, the ARM calibration collects outputs of many tip-curves (>500) satisfying the homogeneity condition during clear-sky to linearly predict the noise diode injection temperature T_{nd} from the temperature of the blackbody target T_{ref}.

PWV from GPS

Water vapor retrieval from GPS is based on the estimation at each receiver of the zenith total delay (ZTD) (Bevis et al. 1992) experienced by the GPS signals while they propagate in the neutral atmosphere. The ZTD is then divided into two components, the zenith hydrostatic delay ZHD and the zenith wet delay ZWD as in Eq.6:

$$ZTD = ZHD + ZWD \quad (6)$$

The ZHD accounts for the hydrostatic component of the atmosphere and can be estimated using the Saastamoinen model (Saastamoinen 1972) if the surface pressure is known; ZWD on the contrary depends entirely on the moisture content of the atmosphere and due to the highly variable humidity profiles, it is poorly predicted from surface measurements only. The ZWD is inferred by subtracting the ZHD from ZTD, and then directly converted in PWV as in Eq.7 by means of the coefficient π (Davis et al. 1985; Bevis et al. 1994) given by Eq. 8.

$$PWV = \pi \cdot ZWD \quad (7)$$

$$\pi = \frac{10^6}{\rho \cdot R_v \left[\left(k_3 / T_m \right) + k_2^{'} \right]} \tag{8}$$

The constants in Eq. 8 are $k_2^{'}$ = 17 K·mb^{-1}, k_3 = 377.600 K^2·mb^{-1} (Davis et al. 1985) ρ is the density of liquid water, Rv is the specific gas constant for water vapor, and T_m (Davis et al. 1985) is the weighted mean temperature of the atmosphere, that is defined in Eq.9:

$$T_m = \frac{\int \left(P_v / T \right) dz}{\int \left(P_v / T^2 \right) dz} \tag{9}$$

where Pv is the partial pressure of water vapor and T is the absolute air temperature. T_m is usually computed from surface temperature T_S (Bevis et al. 1992) considering the strong linear correlation between the two.

CLP Retrieval: A New Approach

In this work we present a single-frequency technique to retrieve CLP by using combined measurements from MWR and GPS. The method is based on considering that the atmospheric opacity τ can be decomposed into the dry opacity τ_d and its components τ_{wet}, due to PWV, and τ_{liq}, due to CLP, by means of the mass absorption coefficients of water vapor k_V and liquid water k_L as in Eq. 10 (Westwater 1993):

$$\tau = \tau_d + \tau_{wet} + \tau_{liq}$$

$$\tau = \tau_d + \kappa_V \cdot \mathrm{PWV} + \kappa_L \, \mathrm{CLP} \tag{10}$$

We can therefore establish a linear relationship between the total opacity computed by the MWR and the water vapor derived by GPS during clear air and for each frequency as in Eq. 11:

$$\begin{aligned} \hat{\tau}_{23CLR} &= c_0 + c_1 \cdot \mathrm{PWV}_{GPS} \\ \hat{\tau}_{31CLR} &= d_0 + d_1 \cdot \mathrm{PWV}_{GPS} \end{aligned} \tag{11}$$

and then compute during cloudy conditions the opacity component τ_{liq} due to the cloud presence as shown in Eq. 12:

$$\tau_{23liq} = \tau_{23} - (c_0 + c_1 \cdot \mathrm{PWV}_{GPS})$$

$$\tau_{31liq} = \tau_{31} - (d_0 + d_1 \cdot \mathrm{PWV}_{GPS}) \tag{12}$$

CPL is obtained by dividing τ_{liq} by the mass absorption coefficient k_L. We considered this method to evaluate the potential of a system composed by a GPS receiver and a possible co-located single channel MWR.

Data Analysis

In our work we considered at first the comparison of PWV from GPS, MWR, and RAOBs to determine its accuracy. We evaluated also the influence that the computation of T_m defined in Eq. 9 in the constant of proportionality π of Eqs. 7 and 8 has on the PWV estimation from GPS. Table 1 shows the PWV from GPS compared to PWV from the MWR C1 and from RAOBs. T_m is computed from surface temperature Ts (Bevis et al. 1992) measured by the co-located surface meteorological sensor. RAOBs were available four times a day at SGP site and were deployed with the new Vaisala RS90 humidity sensor. The comparison with the MWR is presented for both ARM and ETL calibration methods (Liljegren 2000, Han and Westwater 2000), considering thirty minutes averaged MWR measurements centered on GPS data.

Table 1. PWV from GPS compared to PWV from the MWR C1 and RAOBs. MWR C1 is calibrated applying both ETL and ARM algorithm. The PWV retrieval algorithm is based on Rosenkranz (1998). Sample size is 1779 for the comparison with MWR and 202 for the comparison with RAOBs. Bias and standard deviation are referred to PWV(MWR)-PWV(GPS), and PWV(RAOB)-PWV(GPS).

	Bias [cm]	**Std [cm]**
ARM calibration	0.10	0.09
ETL calibration	0.07	0.08
RAOBs	0.02	0.12

In Table 2 we show the same comparison but with T_m computed as in Eq. 9 using water vapor pressure and air temperature profiles as provided by the RAOBs. T_ms were than interpolated to the same sampling time of GPS measurements. Our comparison shows that the computation of T_m from RAOBs improves the rms accuracy of PWV from GPS of the order of 0.01 cm when compared to MWR and RAOBs. For this reason we have adopted this method for the rest of our analysis.

Table 2. PWV from GPS compared to PWV from the MWR C1 and RAOBs. ETL and ARM calibration algorithms are applied to MWR C1. The PWV retrieval algorithm is based on Rosenkranz (1998). Sample size is 1779 for the comparison with MWR and 202 for the comparison with RAOBs. Bias and standard deviation are referred to PWV(MWR)-PWV(GPS), and PWV(RAOB)-PWV(GPS)

	Bias [cm]	**Std [cm]**
ARM calibration	0.09	0.07
ETL calibration	0.06	0.07
RAOBs	0.01	0.10

We then evaluated PWV accuracy in presence of clear air and clouds. Table 3 shows the comparison of PWV from GPS and from MWR E14.

Table 3. Comparison of rms difference between PWV from GPS and from the MWR E14. ARM and ETL calibration methods are considered. The PWV retrieval algorithm is based on Rosenkranz (1998). Sample size is 978 for clear sky and 1280 for cloudy conditions.

PWV rms [cm]			
	Clear-sky	**Cloudy**	**Entire dataset**
ETL calibration	0.066	0.092	0.081
ARM calibration	0.095	0.105	0.100

Clear and cloudy conditions were identified by using ARM product from the Vaisala CT25K ceilometer at SGP site. We classified clear-sky when the ceilometer was indicating clear air for 30 minutes at least.

CLP Retrieval Results

We estimated coefficients c_i and d_i as in Eq. 11 by applying a linear regression to PWV from the GPS dataset and to a thirty minute averaged τ_f from MWR, during clear sky condition as evaluated by the ceilometer. Coefficients for each MWR channel are reported in Table 4, together with mean values of opacities and the standard error (Se) of estimation after the regression.

Table 4. Retrieval coefficients for atmospheric opacities at MWR channels. τ_f mean values and the standard error (Se) of estimation are also reported.

Coef.: c_0, c_1	0.017631 [Np]	0.052785 [Np/cm]
Coef.: d_0, d_1	0.027191 [Np]	0.016413 {Np/cm]
Mean tau_{23}, tau_{31}	0.071500 [Np]	0.043941 [Np]
Se	0.002559 [Np]	0.001535 [Np]

Figure 1 shows CLP time series for April 8, 2003, derived from the MWR C1 applying the standard retrieval algorithm (considering ETL and ARM calibrations) and the method proposed in Eq. 12, CLP time series retrieved at the 31.4 GHz single-channel. The mass absorption coefficient k_L was computed on the basis of the algorithm of Liebe et al. (1991), T_{mr} obtained from RAOBs.

In Figure 2 we present τ_{23} and τ_{31} time series from MWR and from PWV by GPS as in Eq. 11 for the same time period. The corresponding clear air opacities from RAOBs are also shown.

The method proposed retrieves with good accuracy the clear components of τ_{23} and τ_{31} with time series of τ_{23} and τ_{31} from GPS being well correlated to MWR time series during clear skies. The CLP values retrieved show in general less negative values during clear air than CLP from MWR, but they have larger variance especially during cloudy conditions. These initial results show promise, but could be improved perhaps by using GPS data at a sampling rate of fifteen minutes.

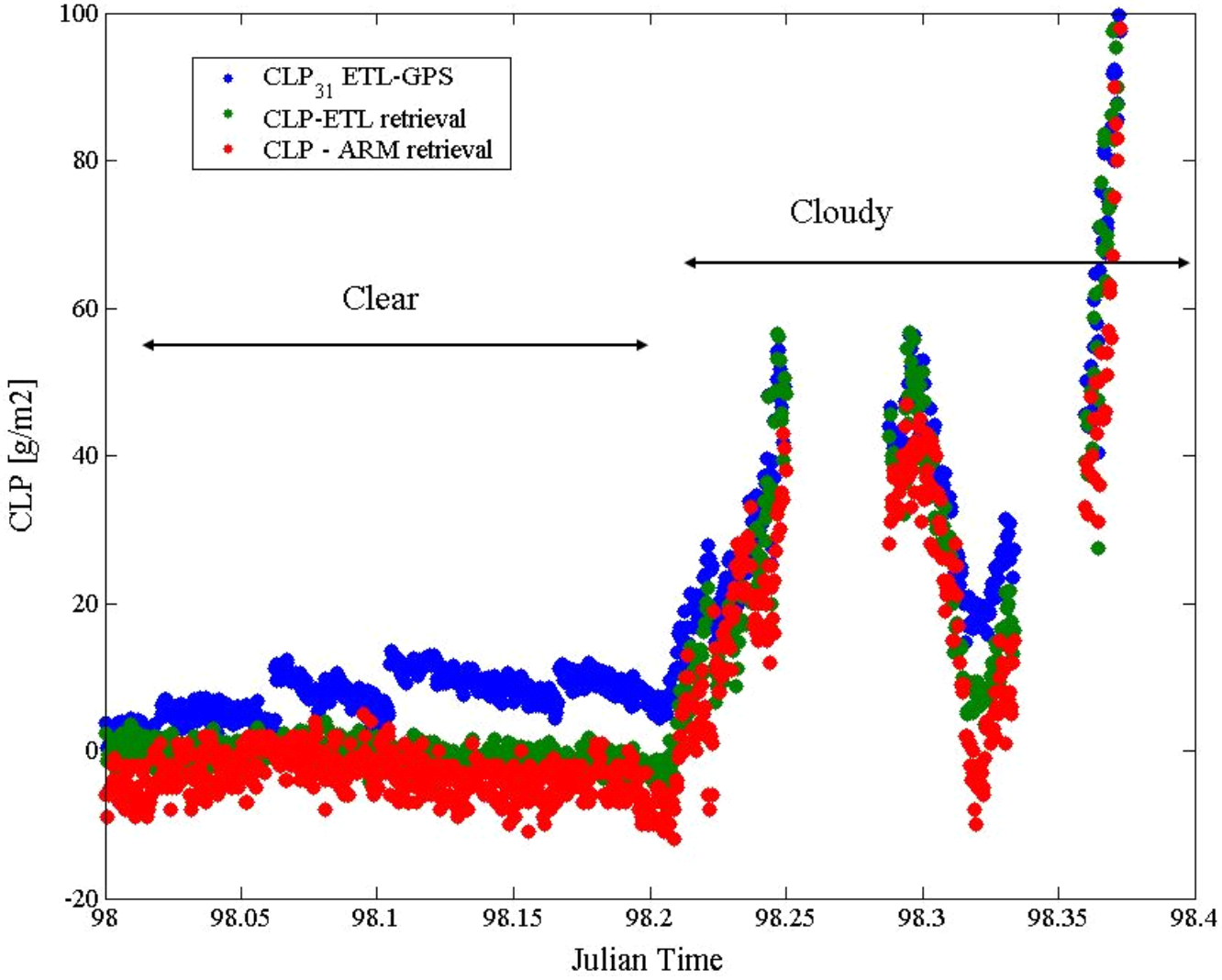

Figure 1. CLP time series for April 8, 2003, derived from the MWR applying the standard retrieval algorithm and ETL calibration (green dots), ARM calibration (red dots) and CLP time series retrieved at the 31.4 GHz single-channel combining GPS and MWR data (blue dots).

Acknowledgement

The work presented in this paper was sponsored by the Environmental Sciences Division of the Department of Energy as a part of their Atmospheric Radiation Measurement Program.

Corresponding Author

Vinia Mattioli, mattioli@diei.unipg.it, Tel. +39-075-5853660

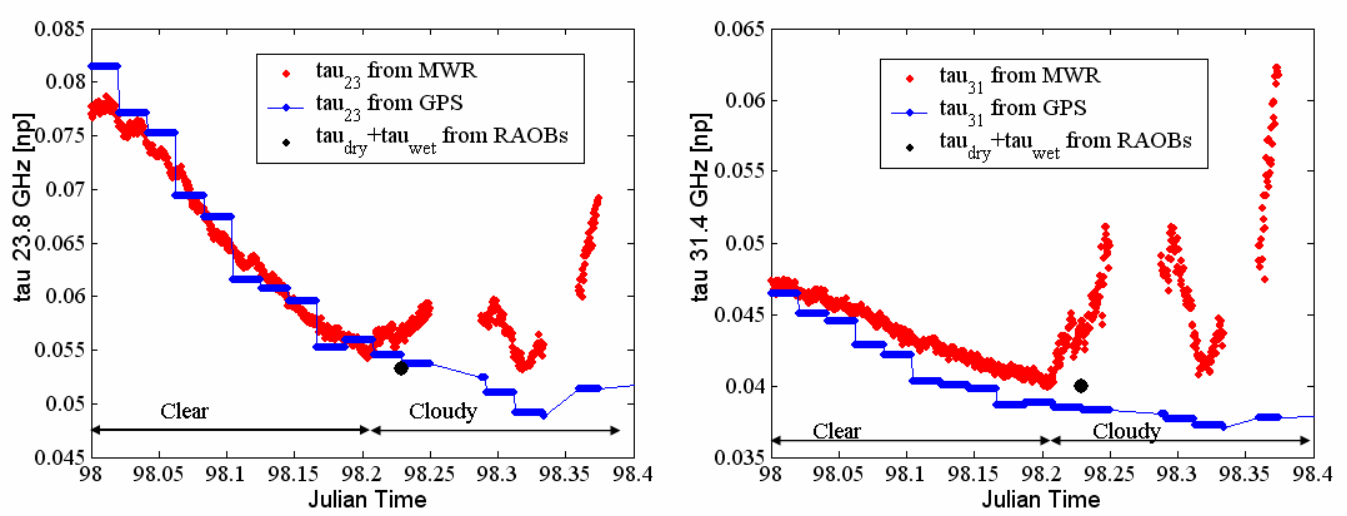

Figure 2. τ_{23} (left) and τ_{31} (right) time series for April 8, 2003, derived from the MWR C1 (red dots), ETL calibration used, and τ_{23} and τ_{31} time series retrieved at the 23.8 GHz and 31.4 GHz by PWV from GPS and the coefficients d_i and c_i reported in Table 4 (blue dots), and corresponding clear air opacities from RAOBs (black dots).

References

Basili, P., S. Bonafoni, R. Ferrara, P. Ciotti, E. Fionda, and R. Ambrosini, 2001: Atmospheric water vapour retrieval by means of both a GPS network and a microwave radiometer during an experimental campaign at Cagliari (Italy) in 1999. *IEEE Trans. Geosci. Rem. Sen.*, **39**(11), 2436–2443.

Bevis, M. S., S. Businger, T. A. Herring, C. Rocken, R. A. Anthes, and R. H. Ware, 1992: GPS meteorology: remote sensing of atmospheric water vapour using the Global Positioning System. *J. Geophys. Res.*, **97**, 787–801.

Bevis, M. S., S. Businger, S. Chiswell, T. A. Herring, R. A. Anthes, C. Rocken, and R. H. Ware, 1994: GPS meteorology: mapping zenith wet delays onto precipitable water. *Journal Applied Meteorol.*, **33**, 379–386.

Davis, J. L., T. A. Herring, I. I. Shapiro, A. E. Rogers, and G. Elgered, 1985: Geodesy by radio interferometry: Effects of atmospheric Modeling Errors on Estimates of Baseline Length. *Radio Sci.*, **20**, 1593–1607.

Han, Y., and E. R. Westwater, 2000: Analysis and improvement of tipping calibration for ground-based microwave radiometers. *IEEE Trans. Geosci. Rem. Sen.*, **38**(3), 1260–1276.

Liebe, H. J., G. A. Hufford, and T. Manabe, 1991: A model for the complex permittivity of water at frequencies below 1 THz. *International Journal of Infrared and Millimeter Waves*, 12(7), 659–675.

Liljegren, J. C., 2000: Automatic self-calibration of ARM microwave radiometers, eds. P. Pampaloni and S. Paloscia. *Microwave Radiometry and Remote Sensing of the Earth's Surface and Atmosphere*, pp. 433-443.

Rocken, C., T. van Hove, J. Johnson, F. Solheim, R. H. Ware, M. Bevis, S. Chiswell, and S. Businger, 1995: GPS/STORM-GPS sensing of atmospheric water vapor for meteorology. *J. Atmos. Oceanic Technol.,* **12**, 468–478.

Rosenkrantz, P. W., 1998: Water vapor microwave continuum absorption: A Comparison of Measurements and Models. *Radio Sci.,* **33**, 919–928.

Saastamoinen, J., 1972: Atmospheric correction for the troposphere and stratosphere in radio ranging of satellites. *The Use of Artificial Satellites for Geodesy*, vol. 15, eds., S. W. Henriksen et al., Geophysics Monograph Series, A.G.U., Washington, D.C.

Westwater, E. R., 1993: Ground-based microwave remote sensing of meteorological variables, *Atmospheric Remote Sensing by Microwave Radiometry*, edited by M. A. Janssen, pp. 145–213, John Wiley, New York.